Pressure- and heat-induced inactivation of butyrylcholinesterase: evidence for multiple intermediates and the remnant inactivation process

Alexandra WEINGAND-ZIADE[1], Fabien RIBES, Frédérique RENAULT and Patrick MASSON[2]

Centre de Recherches du Service de Santé des Armées, Unité d'Enzymologie, BP 87, 38702 La Tronche Cédex, France

The inactivation process of native (N) human butyrylcholinesterase (BuChE) by pressure and/or heat was found to be multistep. It led to irreversible formation of an active intermediate (I) state and a denatured state. This series-inactivation process was described by expanding the Lumry–Eyring [Lumry, R. and Eyring, H. (1954) J. Phys. Chem. **58**, 110–120] model. The intermediate state (I) was found to have a K_m identical with that of the native state and a turnover rate (k_{cat}) twofold higher than that of the native state with butyrylthiocholine as the substrate. The increased catalytic efficiency (k_{cat}/K_m) of I can be explained by a conformational change in the active-site gorge and/or restructuring of the water-molecule network in the active-site pocket, making the catalytic steps faster. However, a pressure/heat-induced covalent modification of native BuChE, affecting the catalytic machinery, cannot be ruled out. The inactivation process of BuChE induced by the combined action of pressure and heat was found to continue after interruption of pressure/temperature treatment. This secondary inactivation process was termed 'remnant inactivation'. We hypothesized that N and I were in equilibrium with populated metastable N′ and I′ states. The N′ and I′ states can either return to the active forms, N and I, or develop into inactive forms, N'_{in} and I'_{in}. Both active N′ and I′ intermediate states displayed different rates of remnant inactivation depending on the pressure and temperature pretreatments and on the storage temperature. A first-order deactivation model describing the kinetics of the remnant inactivation of BuChE is proposed.

Key words: cholinesterase, denaturation of intermediates, temperature.

INTRODUCTION

Two types of cholinesterases (ChE) are present in vertebrates: acetylcholinesterase (AChE, EC 3.1.1.7) and butyrylcholinesterase (BuChE, EC 3.1.1.8). These enzymes are coded by distinct genes and their substrate specificity and sensitivity to inhibitors are different [1]. The essential function of AChE is to terminate the action of the neurotransmitter acetylcholine at cholinergic synapses [1]. Human BuChE, which has no clear physiological function [2,3] shows 51 % sequence identity with human AChE [4]. Cholinesterases are the main target of organophosphorous poisons [5]. Because human BuChE hydrolyses numerous esters, it is of pharmacological and toxicological importance [6–9]. Moreover, recombinant human BuChE is of biotechnological and biomedical interest because some of its mutants could be used as catalytic or pseudocatalytic scavengers against organophosphorous compounds [10,11] and other toxic esters, such as cocaine [12].

ChEs are very efficient catalysts; the rate of acetylcholine hydrolysis by AChE is close to the diffusion-controlled limit [13], and the AChE active site displays ligand-induced conformational adaptability [14]. The active site of ChEs is located at the bottom of a deep [2 nm (20 Å)] and narrow gorge, lined with 14 and eight aromatic residues in *Torpedo californica* (electric ray) AChE [15] and human BuChE [16] respectively. It was shown that the active-site gorge of human BuChE is highly sensitive to environmental conditions and that it plays a key role in the conformational stability and plasticity of the enzyme [17–21]. The denaturing action of hydrostatic pressure on the three-dimensional structure of BuChE is well documented [21–26]. Electrophoresis and 8-anilino-1-naphthalenesulphonate binding under pressure provided evidence for a transition towards a molten-globule state between 1 and 1.6 kbar [22] (1 kbar = 10^8 Pa = 100 MPa). Pressures higher than 2 kbar were found to cause irreversible inactivation/denaturation at 20 °C, followed by subsequent aggregate formation [21]. Fourier-transform IR spectroscopy showed that there is no significant change in secondary structure below 3 kbar; irreversible unfolding occurs at higher pressures and is complete at 8 kbar [$P_{1/2}$ (the midpoint pressure) = 5.5–6 kbar] [26]. The heat denaturation of BuChE has also been extensively investigated. Several studies showed that thermal inactivation of BuChE follows complex first-order kinetics [27,28]. Furthermore, the Eyring ($\ln k/T$ versus $1/T$) plot for enzyme inactivation was found to exhibit a wavelike discontinuity over a span of 2 °C around 58 °C. Non-linear Eyring or Arrhenius ($\ln k$ versus $1/T$) plots may reflect a temperature-induced structural change in the enzyme molecule, and the wavelike transition was interpreted in terms of equilibrium between two temperature-dependent conformational states [27]. Differential scanning calorimetry showed that the midpoint temperature of irreversible thermal denaturation is 62.8 °C at pH 8.0 [20]. As for thermal inactivation at atmospheric pressure (P_0) [27,28], pressure inactivation of BuChE at elevated temperature was found to follow complex kinetics that may be described by the sum of two apparent first-order processes [23]. The inactivation process of BuChE induced by the action of pressure (P) or temperature (T) or their combined action was found to continue after pressure release and/or after stopping heating. This process was termed 'remnant inactivation'. In the present paper a phenomenological analysis of the P/T-induced inactivation process is presented, and a model describing the kinetics of the remnant inactivation of BuChE is proposed.

Abbreviations used: BuChE, butyrylcholinesterase; AChE, acetylcholinesterase; ChE, cholinesterase; BuSCh, butyrylthiocholine iodide; CPO, chlorpyrifos-oxon; P/T, pressure/temperature; N, native human butyrylcholinesterase; I, active intermediate-state butyrylcholinesterase; D, irreversibly denatured-state inactive butyrylcholinesterase; P_0, atmospheric pressure.

[1] Present address: Nestec Research Center, Vers-chez-les-Blanc, CH-1000 Lausanne 26, Switzerland.

[2] To whom correspondence should be addressed (e-mail pymasson@compuserve.com).

MATERIALS AND METHODS

Chemicals

Butyrylthiocholine iodide (BuSCh) and buffer components of biochemical grade were purchased from Sigma. The organophosphate chlorpyrifos-oxon [*O*,*O*-diethyl-*O*-(3,5,6-trichloro-2-pyridinyl) phosphate; CPO] was obtained as an analytical standard (AGR 203674) from Dow Chemical Co. AgroSciences (Indianapolis, IN, U.S.A.).

Enzyme preparation

BuChE was highly purified from human plasma as previously described [25] and stored at 4 °C in 20 mM sodium phosphate buffer, pH 7.0. The enzyme preparation showed a single band corresponding to the BuChE tetramer (G_4; 340 kDa) on both activity- and silver-stained non-denaturing polyacrylamide gels (Figure 1 below). The tetrameric enzyme was homogeneous on isoelectric-focusing gels. The protein concentration in the enzyme preparation was 88 $\mu g \cdot ml^{-1}$ as determined by the bicinchoninic acid method (BCA kit, Pierce, Rockford, IL, U.S.A.). The enzyme specific activity was 115 units $\cdot mg^{-1}$ with BuSCh as the substrate (1 unit hydrolyses 1 μmol of BuSCh/min at pH 7.0 and 25 °C). The active-site concentration as determined by titration with CPO (see below) was 127 nM.

Active-site titration and assay of BuChE

The active-site concentration of BuChE was determined by the method of residual activity using an organophosphate, CPO, as titrant. The titration was carried out as described by Lawler [29] and Leuzinger [30] for AChE. The enzyme activity was determined by the method of Ellman [31] using 1 mM BuSCh in 100 mM sodium phosphate buffer, pH 7.0, at P_0, 22 °C, and at 410 nm, where $\epsilon = 14\,000\ M^{-1} \cdot cm^{-1}$.

P/*T* treatment of the enzyme

Prior to P/T treatments, the enzyme preparation was 3-fold diluted in 20 mM Bis-Tris buffer, pH 7.0. Bis-Tris buffer was chosen because its protonic activity is almost invariant with both the temperature: $dpK_{a(Bis\cdot Tris)}/dT = -0.017\ K^{-1}$ and the pressure $dpH/dP = -0.055\ kbar^{-1}$ [32,33].

The pH change of Bis-Tris buffer induced by increasing the temperature from 25 to 65 °C was calculated to be from 7.0 to 6.78 at P_0 and from 6.68 to 6.46 at 4 kbar. Such small pH changes around neutrality have no significant effect on BuChE stability. For each experiment at a given pressure and temperature, a 150 μl Eppendorf tube was filled with the 3-fold diluted enzyme preparation. Tubes were stopped using a polyethylene stretch film (Parafilm) and were then immersed in the cell compartment of a thermostatically controlled high-pressure vessel. Enzyme samples were subjected to hydrostatic pressure up to 4 kbar between 25 and 70 °C for 30 min. Water was the hydraulic fluid.

Measurements of residual activity

After interruption of P/T treatment, the P/T-treated samples were stored at P_0 at three different temperatures: 0°, 4° and 25 °C. To study the remnant-inactivation process following pressure and/or heat treatments, the residual activity of BuChE was measured by the method of Ellman [31] at P_0 and 22 °C as a function of time from 5 min to 72 h after pressure release and/or temperature lowering. For each assay, 10 μl of P/T-treated enzyme was diluted in 1.5 ml of Ellman's medium. The final BuSCh concentration was 1 mM, so that the rate of BuSCh hydrolysis by BuChE was close to V_{max}. Under our storage-temperature conditions, preliminary experiments showed that the residual activity of BuChE remains unchanged during the 5 min following pressure release.

Detection of enzyme intermediates and denatured states

To detect P/T-induced irreversible enzyme overall conformational changes, non-denaturing electrophoresis in 6 % polyacrylamide gel at pH 8.4 was carried out 24 h after interruption of heating and/or pressurizing as previously described [21]. Gels were silver- or activity-stained. Activity on non-denaturing gels was revealed by the method of Karnovsky and Roots [34], with 1 mM BuSCh as the substrate.

The pI of the native (N) and P/T-treated (intermediate I*) active states was determined by isoelectric focusing on agarose gels (Isogel® 3–10; PeproTech-Tebu, Le Perray-en-Yvelines, France) using a Multiphor II apparatus (Pharmacia, Uppsala, Sweden). The anodic side of the gel was covered by a wick saturated with 0.5 M acetic acid (pH 2.6), and the cathodic side by a wick saturated with 1 M NaOH. The pH gradient was established at 2000 V, 50 mA and 1 W for 10 min. A 5 μl portion of the mixture of markers and 3 μl of 3-fold diluted BuChE preparation (N and I*) were loaded on the cathodic side of the gel using a sample applicator mask. The pI markers (pI 3–10) were purchased from Pharmacia. The isoelectric focusing was carried out at 1500 V, 75 mA and 25 W for 60 min at 15 °C. pI markers were stained with Coomassie Brilliant Blue, and BuChE activity on gel was revealed as described above.

Determination of catalytic parameters

The catalytic behaviour of BuChE with positively charged substrates such as BuSCh can be conveniently described by Scheme 1 and eqn (1) [35–37]:

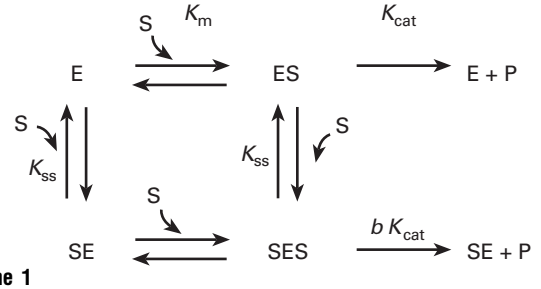

Scheme 1

$$v = \frac{k_{cat}e}{1 + K_m/[S]} \left(\frac{1 + b[S]/K_{ss}}{1 + [S]/K_{ss}} \right) \quad (1)$$

where K_m is the Michaelis–Menten constant, k_{cat} the catalytic constant, e the enzyme active-site concentration, and K_{ss} the dissociation constant of complexes SE and SES ($K_{ss} > K_m$). The productive enzyme–substrate complex (ES) forms when substrate binds to Trp^{82}, the 'anionic' site in the active-site gorge [16]. The enzyme–substrate complex SE corresponds to S bound on the peripheral anionic site located at the rim of the enzyme active-site gorge [36]. When the first substrate molecule is bound to the substrate binding subsite (the choline binding pocket, mainly Trp^{82} and Ala^{328}) of the catalytic site, a second substrate molecule

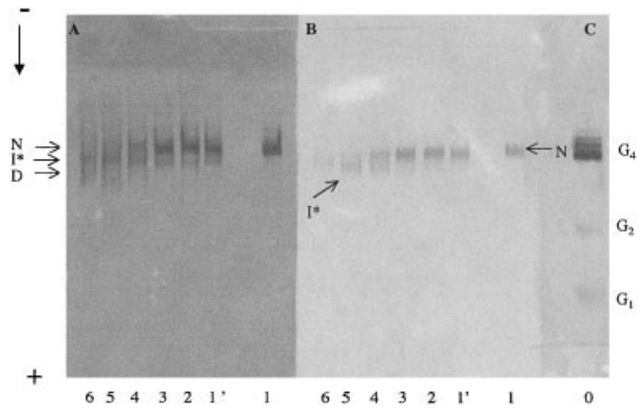

Figure 1 Non-denaturing gel electrophoresis of BuChE

Native wild-type BuChE was submitted to heat (55 °C) for 30 min at different pressures: in (**A**) and (**B**), lanes 1', $P_0 = 0.001$ kbar; lanes 2, 1 kbar; lanes 3, 2 kbar; lanes 4, 3 kbar; lanes 5, 3.5 kbar; lanes 6, 4 kbar. Samples were analysed after 24 h storage at 4 °C at P_0. The control sample (lane 1) is a control containing highly purified native BuChE tetramer at 25 °C. (**A**) photograph of silver-stained gel; (**B**) photograph of activity-stained gel; (**C**) photograph of an activity-stained BuChE sample (lane 0) containing the G_4 (tetramer), G_2 (dimer) and G_1 (monomer) forms of BuChE. N is the native state of BuChE, I* the active intermediate state and D the denatured state.

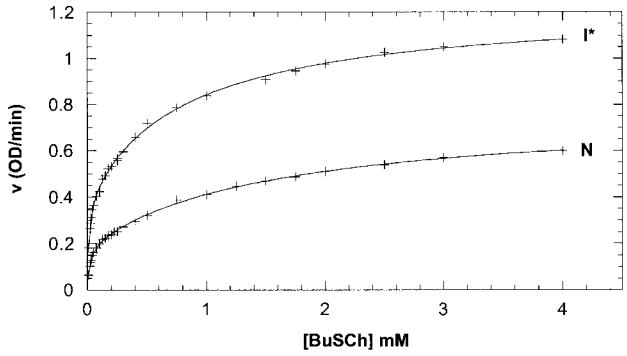

Figure 2 Hydrolysis rate [ΔA_{410}/min) plotted against BuSCh concentration for native (N) and intermediate (I*) BuChE state

The hydrolysis reaction was carried out in 0.1 M phosphate, pH 7.0, at 22 °C; the active-site concentration (e) was 126.6 nM for both enzyme states. OD $\equiv$ *A*.

can bind on to the peripheral anionic site to form the ternary complex, SES. The parameter b reflects the efficiency by which SES forms products. When $b > 1$, there is substrate activation, when $b < 1$ there is substrate inhibition; the enzyme obeys the Michaelis–Menten model if $b = 1$. Wild-type BuChE was found to display substrate activation, showing a b factor close to 3 and $K_{ss} > 10\ K_m$ with BuSCh as the substrate [36,37].

BuChE-catalysed hydrolysis of BuSCh was assayed in 0.1 M phosphate, pH 7.0, at 22 °C using 30 different concentrations of BuSCh ranging from 0.010 to 4 mM. The catalytic parameters were determined by non-linear fitting of eqn (1) using the Sigma plot 4 program (Jandel Scientific, San Rafael, CA, U.S.A.). The active-site concentration (e) as determined by titration with CPO allowed k_{cat} to be calculated from V_{max} ($k_{cat} = V_{max}/e$).

RESULTS AND DISCUSSION

Detection of an intermediate active state and an irreversibly denatured state

The treatment of native (N) BuChE by the combined action of temperature and pressure led to an intermediate active state (I*) and an inactive state, D. I* was seen on both activity- and silver-stained electrophoresis gels. Figure 1 shows typical activity- and silver-stained non-denaturing gels of BuChE samples run 24 h after a 30 min treatment at 55 °C under pressures increasing from P_0 to 4 kbar. The apparent electrophoretic mobility (μ) of these forms ranged as follows: $\mu_D > \mu_I > \mu_N$. The P/T domains of existence of the three enzyme states are indicated in Table 1.

No recovery of activity was observed over the period of time from 5 min to 72 h after treatment, confirming previous findings that P/T-induced inactivation of BuChE was completely irreversible [23,28]. The change in electrophoretic mobility of BuChE after P/T exposure was not due to dissociation of the tetramer (G_4) into dimers (G_2) and monomers (G_1). As seen in Figure 1, the electrophoretic mobility of I* and D does not correspond to the mobility of dimer and monomer. I* and D are tetrameric states. Thus the increased mobility of I* and D compared with N reflects a change in the charge/mass ratio of these species. Along the denaturation reaction pathway of BuChE, it is obvious that numerous intermediate conformations occur between the native and denatured states. These intermediates are transient states of low stability, except the I* state, which is sufficiently stable to be populated. The existence of the I* state accounts for non-linearity of the inactivation kinetics (complex first-order kinetic process, i.e., series-inactivation process) of BuChE caused by heat [28] and pressure [23].

Catalytic parameters of the *P/T*-induced BuChE active intermediate state I*

In order to determine the catalytic parameters of the I* state, BuChE was subjected to a pressure of 4 kbar at 50 °C for 30 min. This treatment caused the total disappearance of the N state, formation of the stable active I* state and a certain amount of denatured D state (see Table 1). Hydrolysis of BuSCh by I* was carried out after 72 h of relaxation at 4 °C. Figure 2 shows

Table 1 Pressure and temperature domains of existence of the different BuChE states

States: N, native; I*, intermediate active; D, denatured. Symbols in square brackets are the relative magnitudes of these states after 30 min treatment.

T (°C)	*P* (kbar)...	0.001	1	2	3	4
25		[N]	[N]	[N]	[N]	[N] < [I*]
50		[N]	[N]	[N]	[N] > [I*]	[I*] > [D]
55		[N] > [I*]	[N] > [I*]	[N] > [I*]	[N] ≈ [I*]	[I*] ≈ [D]
60		[I*] < [D]	[N] ≈ [I*]	[N] ≈ [I*]	[N] ≈ [I*]	[I*] < [D]
65			[I*] < [D]	[I*] < [D]	[I*] < [D]	[I*] ≪ [D]

reaction rates for N and I* plotted against BuSCh concentration at pH 7.0 and 22 °C. The active-site concentration, e, was 126.6 nM for both enzyme states. The catalytic parameters of N and I* were determined by non-linear computer fitting of eqn (1). It is noteworthy that the Michaelis–Menten constant of the I* state is identical with that of the native state ($K_m = 0.021 \pm 0.004$ mM), a value close to K_m reported for the native state under the same conditions [36–38]. The dissociation constant, K_{ss}, of complexes SE and SES (binding of the second substrate molecule on the peripheral anionic site) is nearly unchanged for the I* state, 1.29 ± 0.13 mM compared with 2.59 ± 0.51 mM for the N state. Titration of the active-site concentration (e) of N and I* samples allowed k_{cat} to be determined. The catalytic constant of I* was $54\,500 \pm 500$ min^{-1} compared with $27\,000 \pm 1000$ min^{-1} for the N state. The twofold increase in k_{cat} indicates that the catalytic steps were altered in I* compared with the N state. However, as for the native BuChE [37], the I* state displayed activation by excess substrate at moderate substrate concentration higher than 0.2 mM, and the value of the b factor remained unchanged (3.87 ± 0.05 for the N state and 3.29 ± 0.36 for the I* state). This indicates that the relative efficiency of the ternary complex SES to acylate and deacylate BuSCh was not altered. As previously reported, BuChE subjected to ultrasound showed a 20 % increase in enzyme activity during the first 5 min of irradiation, followed by the inactivation phase [19]. This transient increase in BuChE activity was interpreted as the result of formation of an intermediate more active than the N state. Similarly, heating of *Bungarus fasciatus* (banded krait) venom AChE at 45 °C generated an intermediate state more active than the native state [38].

At moderate substrate concentrations ([S] < K_{ss}), the catalytic properties of the N and I* states can be interpreted according to the model of three-step binding leading to the acyl-enzyme intermediate [36] (Scheme 2):

$$E + S \underset{K_s}{\rightleftharpoons} ES_1 \underset{K_I}{\rightleftharpoons} ES_2 \underset{K_{II}}{\rightleftharpoons} ES_3 \xrightarrow{K_2} EA + P_1 \xrightarrow{K_3} E + P_2$$

Scheme 2

In the above Scheme, ES_1, ES_2 and ES_3 are enzyme–substrate complexes. The first complex (ES_1) involves interactions between the quaternary ammonium group of BuSCh and the peripheral site (Asp^{70} and Tyr^{332}) [36,39]. The second intermediate (ES_2) corresponds to the substrate positioned in the gorge between Asp^{70} and Trp^{82}. In the third complex (ES_3), the substrate is positioned at the bottom of the gorge, in the catalytic site, in a conformation suitable for the nucleophilic attack. EA is the acylated enzyme intermediate, and P_1 and P_2 are products. K_s is the dissociation constant of the ES_1 complex, K_I and K_{II} are the isomerization constants of the ES_2 and ES_3 complexes, respectively. The expressions for K_m, k_{cat} and the apparent bimolecular constant, k_{cat}/K_m, derived from Scheme 2, are:

$$k_{cat} = \frac{k_2}{K_I K_{II} + K_{II} + \frac{k_2}{k_3} + 1} \quad (2)$$

$$K_m = \frac{K_s K_I K_{II}}{K_I K_{II} + K_{II} + \frac{k_2}{k_3} + 1} \quad (3)$$

$$\frac{k_{cat}}{k_m} = \frac{k_2}{K_s K_I K_{II}} \quad (4)$$

Accordingly, the fact that there was no difference in K_m between the N and I* states, suggests that K_S, K_I and K_{II} of I* were not altered compared with N. On the contrary, k_{cat} and the apparent bimolecular constant (k_{cat}/K_m) of I* were twice as high as the catalytic constants for N. This indicates that the twofold increase in the catalytic efficiency of I* results from a twofold increase in the rate constant of acylation (k_2). Increase in k_2 is realized by lowering the energy barrier of the activated complex, $ES_3^{\neq}$. Such a situation corresponds to enzyme-transition-state complementarity: the energy of the enzyme–substrate complex (ES_3) is the same for N and I*. So that, for I*, the binding energy is realized only in the transition-state complex, $I^*S_3^{\neq}$. Hydrostatic pressure is known to induce protein conformation changes and hydration changes at protein/solvent interfaces [40,41]. Thus the stability of the transition states ($I^*S_3^{\neq}$ and $IA^{\neq}$) may be increased by restructuring the network of water molecules in the active-site gorge. Such a pressure-stabilizing effect was seen for the dealkylation reaction ('aging') of phosphorylated BuChE [20]. However, because site-directed mutagenesis of residues remote from the active site was found to alter BuChE-catalysed reactions [20,39], a concomitant irreversible conformational change in the active-site gorge making the catalytic steps easier cannot be ruled out.

pI of the *P*/*T*-induced BuChE active intermediate state I*

The pI of the I* state was found to be 0.2 pH unit above the pI of the native state (pI = 4.3). This pI change can be interpreted as the result of a slight conformational change modifying the electric properties of the enzyme surface. Molecular-dynamics simulations of human BuChE at elevated pressure (from 1 to 3 kbar) showed a decrease in the molecular volume (J. Stojan and P. Masson, unpublished work), which is consistent with a conformational change resulting from the collapse of cavities and packing reorganization.

P/*T*-induced covalent modifications of the enzyme cannot be ruled out. However, the fact that $pI_{(I^*)} > pI_{(N)}$ indicates that, if a chemical modification occurred, it was neither a deamidation of surface-exposed Gln/Asn nor a desialylation of glycan chains. Among possible *P*/*T*-favoured covalent modifications is the Maillard reaction, leading to glycation of advanced end products.

Proposed mechanism of *P*/*T*-induced BuChE inactivation

The general mechanism of protein/enzyme denaturation/inactivation proposed by Lumry and Eyring (Scheme 3) [42] can be applied to BuChE. Accordingly, inactivation of BuChE under $P \geqslant 4$ kbar at $T \geqslant 65$ °C (Table 1) can be depicted by the two-step model (Scheme 3):

$$N \underset{k_{-1}}{\overset{k_1}{\rightleftharpoons}} N'_{(P,T)} \xrightarrow{k_2} D_{(P,T)}$$

Scheme 3

Where N is the native state, $N'_{(P,T)}$ is a partially and reversibly unfolded state, and $D_{(P,T)}$ the irreversibly inactivated form of the enzyme.

Inactivation under $P < 4$ kbar and $T < 65$ °C follows a more complex kinetics, because it involves the stable intermediate I* (Table 1). I*, detected on gels, was assumed to be composed of the stable active state (I) in rapid equilibrium with a state [$I'_{(P,T)}$].

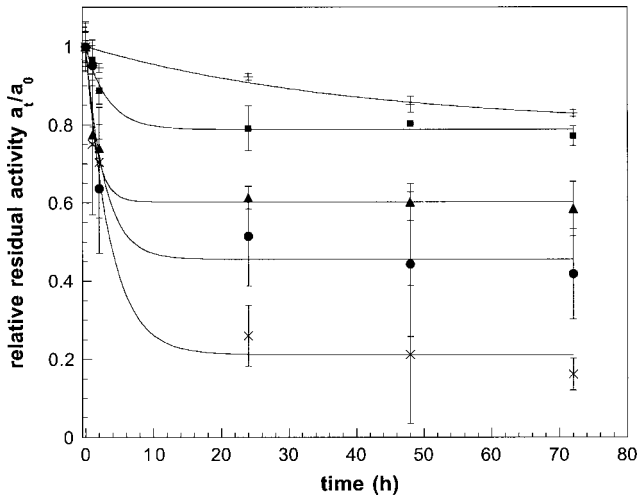

Figure 3 Change in residual activity of BuChE as a function of storage time at 4 °C following treatment at 55 °C for 30 min under 0.001 kbar (+), 1 kbar (▲), 2 kbar (●), 3 kbar (■) and 4 kbar (×)

Measurements of the remaining activity were carried out at pH 7.0, 22 °C and P_0. The symbol '+' is somewhat masked by the error bar.

Thus the P/T-induced inactivation processes of BuChE can be described by an expanded Lumry–Eyring model (Scheme 4):

$$N \underset{k_{-1}}{\overset{k_1}{\rightleftharpoons}} N'_{(P,T)} \xrightarrow{k_i} I_{(P,T)} \underset{k_{-2}}{\overset{k_2}{\rightleftharpoons}} I'_{(P,T)} \xrightarrow{k_D} D_{(P,T)}$$

Scheme 4

Thermal inactivation of monomeric AChE from *B. fasciatus* was also found to obey this model [38].

Remnant inactivation of BuChE

When native BuChE (N) was heated to $T \geqslant 50$ °C at P_0, or under $P \geqslant 4$ kbar at 25 °C, or subjected to the combined action of heat ($T = 50$ °C) and high pressure ($P \geqslant 2$ kbar), the inactivation of BuChE was found to continue after decompression and/or lowering the temperature. This remnant inactivation process was puzzling.

Unlike what was seen during the time course of P/T inactivation, no change either in the mobility or quaternary structure of active BuChE tetramers (N and I* states) was detectable by non-denaturing gel electrophoresis during the remnant-inactivation process, even after a relaxation time of 72 h. This suggests that the fine structural changes occurring during the remnant-inactivation process are likely to be located in the active-site gorge. It should be remembered that the active-site gorge was shown to be very sensitive to environmental perturbations [18–21,23] and that mutations or chemical modifications of specific active gorge residues were found to affect the conformational stability of BuChE [20,21].

Kinetics of the remnant inactivation

Figure 3 shows a typical remnant-inactivation time course of BuChE stored at 4 °C after 30 min treatment at 55 °C under different pressures. Taking a_0 as the residual activity of BuChE 5 min (t_0) after P/T treatment and a_t as the residual activity of BuChE at different times t varying from 5 min to 72 h, the change in relative residual activity a_t/a_0 versus time describes the remnant-inactivation kinetic process. As can be seen, the residual activity of BuChE decreased progressively as a function of relaxation time. After treatment at $P \geqslant 1$ kbar, a_t/a_0 did not change beyond 24 h and up to 72 h. Therefore the denaturing process of BuChE induced by P and T must be regarded as the sum of two phenomena: (a) the inactivation under P/T, leading to I* and D, and (b) the remnant inactivation of P/T-treated enzyme at P_0 after decompression and chilling.

In the proposed mechanism of inactivation (Scheme 4), N and N′ as well as I and I′ are in rapid equilibrium displaced towards N′ and I′ respectively ($K_1 = k_1/k_{-1}$ and $K_2 = k_2/k_{-2}$ are high). Assuming that $k_i \ll k_{-1}$ and $k_D \ll k_{-2}$, there is accumulation of N′ and I′ during the inactivation process. $N'_{(P,T)}$ and $I'_{(P,T)}$ are a continuum of metastable intermediates which are susceptible to develop in two ways: they can either return to the active states $N_{(P,T)}$ and $I_{(P,T)}$ or be converted into inactive states, N'_{in} and I'_{in} through the remnant inactivation process (Scheme 5). After ceasing the P/T treatment, gel electrophoresis failed to show that N′ was converted into I*, even after 5-day storage at P_0. This suggests that a high-energy barrier exists between the N′ and I conformational forms under standard conditions of P/T. Thus, after interrupting the P/T treatment, the remnant-inactivation process, due to the populated states N′ and I′, can be depicted by the two parallel right reactions in Scheme 5:

$$\begin{cases} N \underset{}{\overset{k'_{-1}}{\leftarrow}} N'_{(P,T)} \xrightarrow{k'_{1in}} N'_{in} \\ I_{(P,T)} \underset{}{\overset{k'_{-2}}{\leftarrow}} I'_{(P,T)} \xrightarrow{k'_{2in}} I'_{in} \end{cases}$$

Scheme 5

Accordingly, the kinetics of remnant inactivation can be described by the equation rate of a biexponential process with two first-order rate constants k'_{1in} and k'_{2in}:

$$a_t - a_\infty = N'_{(P,T)0}\exp(-k'_{1in}t) - I'_{(P,T)0}\exp(-k'_{2in}t) \quad (5)$$

where a_∞ is the residual activity of active states $N_{(P,T)}$ and $I_{(P,T)}$ after full consumption of the $N'_{(P,T)}$ and $I'_{(P,T)}$ species. For a phenomenological analysis, this integrated rate expression may be simplified by an apparent first-order process defined by two parameters [43]:

$$a_t/a_0 = (1-\alpha)\exp(-kt) + \alpha \quad (6)$$

where $\alpha = a_\infty/a_0$ and k is the apparent overall remnant-inactivation rate constant, a composite constant including k'_{1in} and k'_{2in}. The Marquadt method of iterative convergence [44] was used to calculate the best values of k and α. For instance, as seen in Figure 3, eqn (6) fitted the data for the remnant-inactivation process at 4 °C of P/T-treated enzyme.

For P/T-treated enzyme up to 50 °C, whatever the pressure treatment, α was found to decrease slightly (e.g., $\alpha = 1$, 0.8 and 0.7 for $P = P_0$, 2 kbar and 3 kbar respectively), but it dramatically decreased for treatments at $T > 50$ °C (e.g., $\alpha = 0.2$ at 65 °C and any pressure).

k for remnant inactivation at 4 °C was plotted against the treatment temperature (50 to 65 °C) at different P values (< 4 kbar) (Figure 4). Following heat treatment at P_0, there was no remnant inactivation, except when the enzyme was heated at 50 °C ($k = 0.2\ h^{-1}$). Following treatment at 1 kbar/55 °C, where both native and intermediate enzyme forms were populated with [N] > [I*], k was 0.7 h^{-1}. Higher pressures (2 and 4 kbar) caused a progressive increase in k with temperature ($k = 1.4\ h^{-1}$ at

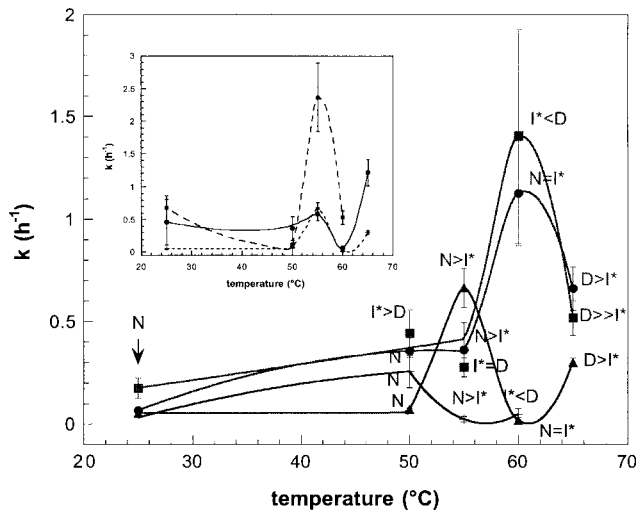

Figure 4 Change in the overall rate constant of remnant inactivation (*k*) at 4 °C as a function of the temperature of treatment at different pressures

BuChE was submitted to heat (from 50 to 65 °C) for 30 min at different pressures: +, 0.001 kbar; ▲, 1 kbar; ●, 2 kbar; ■, 4 kbar. The inset shows *k* as a function of temperature of treatment at 1 kbar for 30 min and at different temperatures of storage: 0 °C (—●—); 4 °C (- - + - -) and 25 °C (– – ■ – –).

60 °C) and then decreased to $k = 0.5$–0.7 h^{-1} at 65 °C. Treatments at 4 kbar and temperatures ranging between 50° and 65 °C caused the disappearance of the N state; the generated I* state was the only active enzyme form. The change in k correlated with the relative amount of N and I* (Figure 4) (which depends on the P/T conditions of treatment, cf. Table 1) indicates that the I′ state was more susceptible to remnant inactivation than the N′ state, i.e. k_{2in} k_{1in}.

The rate of remnant inactivation was also determined for P/T-treated BuChE stored at 25° and 0 °C (inset to Figure 4). After 30 min treatment at 1 kbar/55 °C, the higher value of k was for storage at 25 °C. Under these treatment conditions, the amount of generated N′ state was presumably higher than that of the I′ state. The high value of k (2.4 h^{-1}) at 25 °C, indicates that, at this temperature, N′ and I′ (Scheme 5) were converted predominantly into inactive states N'_{in} and I'_{in}. This provides evidence that the storage temperature controls the rate of remnant inactivation.

During the inactivation process, depending on the P/T conditions, there is formation of a particular metastable state among the continuum of forms N'_1, N'_2, N'_3 ... N'_n and I'_1, I'_2, I'_3 ... I'_n. Each metastable state is susceptible to undergoing remnant inactivation at a rate constant depending on storage temperature. Thus the observed overall rate constant, k, is the result of the contribution of numerous individual rate constants. Therefore the interpretation of plots of k versus treatment temperature at different pressures is not straightforward. The energetics of the remant inactivation is also intriguing. This phenomenon calls to mind conformational fluctuations and drift of proteins subjected to cryoinactivation or pressure treatment [45,46]. However, unlike the conformational drift described by Weber and his colleagues for oligomeric enzymes, where dissociated subunits are drifted [47,48], in the case of the remnant inactivation of BuChE, there is no evidence for transient dissociation of the tetrameric enzyme. Thus it may be stated that the N′ and I′ states generated from the active states (N and I) of BuChE during the P/T treatment encountered a lower energy barrier toward the N'_{in} and I'_{in} states than toward the N and I states upon depressurization and chilling.

Conclusion

The process of native (N) BuChE inactivation by pressure and/or heat led to several enzyme states: an active intermediate state (I*) and a denatured state (D). The intermediate state (I*) was found to have a higher catalytic efficiency, which can be tentatively explained by a change in the hydration of the active site and/or a conformational change in the active-site gorge accounting for transition-state stabilization.

The remnant inactivation following P/T treatments suggests that both N and I were in equilibrium with a continuum of metastable intermediates, N′ and I′, susceptible to inactivation upon storage. The rate of remnant inactivation was found to depend on the P/T treatments as well as the storage temperature after these treatments. Results indicated that the rate of remnant inactivation of the I′ state is faster than that of the N′ state. The instability of the N′ and I′ conformational states likely results from subtle conformation and hydration changes in the active-site gorge. The recent determination of the X-ray structure of human BuChE (Y. Nicolet, F. Nachon, P. Masson, J. Fontecilla-Camp and O. Lockridge, unpublished work), gives us the opportunity of studying the effect of pressure on the crystal structure of BuChE. Although the compressibility of solution enzymes, a flexibility parameter, is related to thermal fluctuations, the pictures of the crystal enzyme at elevated pressures are expected to shed light on the location of voids and pressure-sensitive domains affecting the functionality of the active-site gorge of BuChE.

This work was supported by the Direction des Systèmes de forces et de la Prospective/Service Technique des Technologies Communes (DSP/STTC; grant no. 97/08). A. W.-Z. was in receipt of a fellowship from the Nestec Research Center, Lausanne, Switzerland.

REFERENCES

1 Massoulié, J, Pezzementi, L., Bon, S., Krejci, E. and Vallette, F. (1993) Molecular and cellular biology of cholinesterases. Prog. Neurobiol. **41**, 31–91
2 Chatonnet, A. and Lockridge, O. (1989) Comparison of butyrylcholinesterase and acetylcholinesterase. Biochem. J. **260**, 625–634
3 Mack, A. and Robitzki, A. (2000) The key role of butyrylcholinesterase during neurogenesis and neural disorders: an antisense-5′ butyrylcholinesterase–DNA study. Prog. Neurobiol. **60**, 607–628
4 Soreq, H. E., Ben-Aziz, R., Prody, C. A., Seidman, S., Gnatt, A., Neville, L., Lieman-Hurwitz, J., Lev-Lehman, E., Ginzberg, D., Lapidot-Lifson, Y. and Zakut, H. (1990) Molecular cloning and construction of the coding region for human acetylcholinesterase reveals a G + C-rich attenuating structure. Proc. Natl. Acad. Sci. U.S.A. **87**, 9688–9692
5 Ballantyne, B. and Marrs, T. C. (1992) Clinical and Experimental Toxicology of Organophosphates and Carbamates, Butterworth-Heinemann, Oxford
6 Lockridge, O. (1992) Genetic variants of human serum butyrylcholinesterase influence the metabolism of the muscle relaxant sucinylchloine. In Pharmacogenetics of Drug Metabolism (Kalow, W., ed.), pp. 15–50, Pergamon Press, New York
7 Mattes, C. E., Belendiuk, G. W., Lynch, T. J., Brady, R. O. and Dretchen, K. L. (1998) Butyrylcholinesterase: an enzyme antidote for cocaine intoxication. Addict. Biol. **3**, 23–40
8 Morton, C. L., Wadkins, R. M., Danks, M. K. and Potter, P. M. (1999) The anticancer prodrug CPT-11 is a potent inhibitor of acetylcholinesterase but is rapidly catalyzed to SN-38 by butyrylcholinesterase. Cancer Res. **59**, 1458–1463
9 Carmona, G. N., Jufer, R. A., Goldberg, S. R., Gorelick, D. A., Greig, N. H., Yu, Q.-S., Cone, E. J. and Schindler, C. W. (2000) Butyrylcholinesterase accelerates cocaine metabolism: *in vitro* and *in vivo* effects in nonhuman primates and humans. Drug Metab. Dispos. **28**, 367–371

10 Raveh, L., Grunwald, J., Marcus, D., Papier, Y., Cohen, E. and Ashani, Y. (1993) Human butyrylcholinesterase as a general prophylactic antidote for nerve agent toxicity: *in vitro* and *in vivo* quantitative characterization. Biochem. Pharmacol. **45**, 2465–2474

11 Broomfield, C. A., Lockridge, O. and Millard, C. B. (1999) Protein engineering of a human enzyme that hydrolyzes V and G nerve agents: design, construction and characterization. Chem.–Biol. Interact. **119/120**, 413–418

12 Xie, W., Varkey Altamirano, C., Bartels, C. F., Speirs, R. J., Cashman, J. R. and Lockridge, O. (1999) An improved cocaine hydrolase: The A328Y mutant of human butyrylcholinesterase is 4-fold more efficient. Mol. Pharmacol. **55**, 83–91

13 Quinn, D. M. (1987) Acetylcholinesterase: enzyme structure, reaction dynamics, and virtual transition states. Chem. Rev. **87**, 955–979

14 Rosenberry, T. L. (1975) Acetylcholinesterase. Adv. Enzymol. Relat. Areas Mol. Biol. **43**, 103–218

15 Sussman, J. L., Harel, M., Frolow, F., Oefner, C., Goldman, A., Toker, L. and Silman, I. (1991) Atomic structure of acetylcholinesterase from *Torpedo californica*: A prototypic acetylcholine-binding protein. Science **253**, 872–879

16 Harel, H., Sussman, J. L., Krejci, E., Bon, S., Massoulié, J. and Silman, I. (1992) Conversion of acetylcholinesterase to butyrylcholinesterase: modeling and mutagenesis. Proc. Natl. Acad. Sci. U.S.A. **89**, 10827–10831

17 Masson, P. and Balny, C. (1990) Conformational plasticity of butyrylcholinesterase as revealed by high pressure experiments. Biochim. Biophys. Acta **1041**, 223–231

18 Levitsky, V., Xie, W., Froment, M. T., Lockridge, O. and Masson, P. (1999) Polyol-induced activation by excess substrate of the D70G butyrylcholinesterase mutant. Biochim. Biophys. Acta **1429**, 422–430

19 Froment, M. T., Lockridge, O. and Masson, P. (1998) Resistance of butyrylcholinesterase to inactivation by ultrasound: effects of ultrasound on catalytic activity and subunit association. Biochim. Biophys. Acta **1387**, 53–64

20 Masson, P., Cléry, C., Guerra, P., Redslob, A., Albaret, C. and Fortier, P. L. (1999) Hydration change during the aging of phosphorylated human butyrylcholinesterase: importance of residues D70 and E197 in the water network as probed by hydrostatic and osmotic pressures. Biochem. J. **343**, 361–369

21 Masson, P., Gouet, P. and Cléry, C. (1994) Pressure and propylene carbonate denaturation of native and ''aged'' phosphorylated cholinesterase. J. Mol. Biol. **238**, 466–478

22 Cléry, C., Renault, F. and Masson, P. (1995) Pressure-induced molten globule state of cholinesterase. FEBS Lett. **370**, 212–214

23 Weingand-Ziadé, A., Renault, R. and Masson, P. (1997) Combined-pressure/heat-induced inactivation of butyrylcholinesterase. Biochim. Biophys. Acta **1340**, 245–252

24 Weingand-Ziadé, A., Renault, F. and Masson, P. (1999) Differential effect of pressure and temperature on the catalytic behaviour of wild-type human butyrylcholinesterase and its D70G mutant. Eur. J. Biochem. **264**, 327–335

25 Cléry, C., Bcc, N., Balny, C., Mozhaev, V. V. and Masson, P. (1995) Kinetics of butyrylcholinesterase in reversed micelles under high pressure. Biochim. Biophys. Acta **1253**, 85–93

26 Cléry, C., Goossens, K., Hui Bon Hoa, G., Heremans, K., Balny, C. and Masson, P. (1993) Pressure-induced structural modifications of butyrylcholinesterase. In Stability and Stabilization of Enzymes (van den Twell, W. J. J., Harder, A. and Buitelaar, R. M., eds.), pp. 255–260, Elsevier, Amsterdam

27 Cauet, G., Friboulet, A. and Thomas, D. (1987) Substrate activation and thermal denaturation kinetics of the tetrameric and the trypsin-generated monomeric forms of horse serum butyrylcholinesterase. Biochim. Biophys. Acta **912**, 338–342

28 Masson, P. and Laurentie, M. (1988) Stability of butyrylcholinesterase: thermal inactivation in water and deuterium oxide. Biochim. Biophys. Acta **957**, 111–121

29 Lawler, C. (1961) Turnover time of acetylcholinesterase. J. Biol. Chem. **236**, 2296–2301

30 Leuzinger, W. (1971) The number of catalytic sites in acetylcholinesterase. Biochem. J. **123**, 139–141

31 Ellman, G. L., Courtney, K. D., Andres, V. and Featherstone, R. M. (1961) A new and rapid colorimetric determination of acetylcholinesterase activity. Biochem. Pharmacol. **7**, 88–95

32 Kitamura, Y. and Itoh, T. (1987) Reaction volume of protonic ionization for buffering agent. Prediction of pressure dependence of pH and pOH. J. Solution Chem. **16**, 715–725

33 Goldbeck, A., Lechner, M. D., Witz, J., Nordmeier, E. and Ibel, K. (1991) The thermal stability of turnip yellow mosaic virus under hydrostatic pressure. Eur. Biophys. J. **20**, 151–156

34 Karnovsky, M. J. and Roots, L. (1964) A ''direct-coloring'' thiocholine method for cholinesterases. J. Histochem. Cytochem. **12**, 219–221

35 Radic, Z., Pickering, N. A., Vellom, D. C., Camp, S. and Taylor, P. (1993) Three distinct domains in the cholinesterase molecule confer selectivity for acetyl- and butyrylcholinesterase inhibitors. Biochemistry **32**, 12074–12084

36 Masson, P., Legrand, P., Bartels, C. F., Froment, M. T., Schopfer, L. M. and Lockridge, O. (1997) Role of aspartate 70 and tryptophan 82 in binding of succinyldithiochioline to human butyrylcholinesterase. Biochemistry **36**, 2266–2277

37 Masson, P., Froment, M. T., Bartels, C. F. and Lockridge, O. (1996) Asp 70 in the peripheral anionic site of human butyrylcholinesterase. Eur. J. Biochem. **235**, 36–48

38 Rochu, D., Georges, C., Répiton, J., Viguié, N., Saliou, B., Bon, C. and Masson, P. (2001) Thermal stability of acetylcholinesterase from *Bungarus fasciatus* venom as investigated by capillary electrophoresis. Biochim. Biophys. Acta **1545**, 216–226

39 Masson, P., Xie, W., Froment, M. T., Levitsky, V., Fortier, P. L., Albaret, C. and Lockridge, O (1999) Interaction between the peripheral site residues of human butyrylcholinesterase, D70 and Y332, in binding and hydrolysis of substrates. Biochim. Biophys. Acta **1433**, 281–293

40 Mozhaev, V. V, Heremans, K., Frank, J., Masson, P. and Balny, C. (1996) High pressure effects on protein structure and function. Protein Struct. Funct. Genet. **24**, 81–91

41 Michels, P. C., Hei, D. and Clark, D. S. (1996) Pressure effects on enzyme activity and stability at high temperatures. Adv. Prot. Chem. **48**, 341–376

42 Lumry, R. and Eyring, H. (1954) Conformational changes of proteins. J. Phys. Chem. **58**, 110–120

43 Sadana, A. and Henley, J. P. (1987) Single-step unimolecular non-first-order enzyme deactivation kinetics. Biotechnol. Bioeng. **30**, 717–723

44 SAS Institute (1982) SAS Users Guide: Statistics Edition, SAS Institute Inc., Cary, NC

45 Cooper, A. (1988) Conformational change, fluctuation and drift in biological macromolecules: an empirical Langevin approach. J. Mol. Liquids **39**, 195–206

46 Weber, G. (1989) Dynamics of oligomeric proteins. J. Mol. Liquids **42**, 255–268

47 Silva, J. L., Miles, E. W. and Weber, G. (1986) Pressure dissociation and conformational drift of the β dimer of tryptophan synthase. Biochemistry **25**, 5780–5786

48 Ruan, K.-C. and Weber, G. (1989) Hysteresis and conformational drift of pressure-dissociated glyceraldehydephosphate dehydrogenase. Biochemistry **28**, 2144–2153

Received 14 February 2000/22 January 2001; accepted 7 March 2001